The SMC as a probe of dust in the early Universe

Principal Investigator: Gregory C. Sloan
Institution: Cornell University
Electronic mail: sloan@isc.astro.cornell.edu
Technical Contact: Gregory C. Sloan, Cornell University
Co−Investigators: Jeronimo Bernard−Salas, Cornell Univ.
Robert Blum, NOAO
Alberto Bolatto, Univ. of Maryland
Caroline Bot, Caltech
Martin Cohen, Univ. of California at Berkeley
Karl Gordon, STScI
Joseph Hora, Harvard−Smithsonian CfA
Remy Indebetouw, Univ. of Virginia
Luke Keller, Ithaca College
Kathleen Kraemer, Air Force Research Laboratory
Eric Lagadec, Manchester Univ.
Vianney Lebouteiller, Cornell Univ.
Aigen Li, Univ. of Missouri
Sue Madden, CEA/Saclay
Massimo Marengo, Harvard−Smithsonian CfA
Mikako Matsuura, NAO of Japan
Franciska Markwick−Kemper, Manchester Univ.
Margaret Meixner, STScI
Joana Oliveira, Univ. of Keele
Karin Sandstrom, Univ. of California at Berkeley
Marta Sewilo, STScI
Josh Simon, Caltech
Angela Speck, Univ. of Missouri
Alexander Tielens, NASA Ames Research Center

Schuyler van Dyk, SSC/Caltech
Jacco van Loon, Univ. of Keele
Kevin Volk, Gemini Observatory
Peter Wood, Australian National Univ.
Albert Zijlstra, Manchester Univ.
James Houck, Cornell Univ.

Science Category: Extragalactic: local group galaxies

Observing Modes: IRS Staring, IRS Mapping, MIPS SED

Hours Requested: 54.2

Proprietary Period(days): 365

Abstract:
We propose a comprehensive spectroscopic survey of the Small Magellanic Cloud (SMC), using the IRS and MIPS−SED. The SMC has a metallicity similar to high−redshift galaxies, and its proximity makes it a spatially resolved proxy for star−forming galaxies in the distant, early Universe. The sensitivity of the Spitzer Space Telescope allows us to to observe dust in nearly every stage of its life cycle in the SMC so that we can study how the interactions of dust and its host galaxy differ from more metal−rich systems like the Galaxy and the LMC. Our proposed observations concentrate on important classes underrepresented in the archive of SMC spectra such as young stellar objects, compact H II regions, objects in transition to and from the asymptotic giant branch, and supergiants. These observations, in combination with those already in the archive, will give us a complete picture of the dust in a metal−poor star−forming galaxy similar to those in the early Universe. We request 116 hours, 62 as IRS GTO time and 54 as GO time.

1 Scientific Justification

We propose to complete a comprehensive spectral study of the dust inventory of the Small Magellanic Cloud (SMC) using the IRS on the *Spitzer Space Telescope*. This study fills key gaps in existing samples by targeting representative objects in all stages of the life cycle of dust, including sources injecting dust into the interstellar medium (ISM) and sources forming from that dust, and it will use both the IRS (108.4 hrs) and MIPS in SED mode (7.8 hrs). In this proposal, we are requesting a total of 54.2 hours of GO time. The IRS Team has allocated 62 hours of their GTO time to this survey, and we are requesting that time in a separate, but otherwise identical, proposal.

1.1 Introduction

Dust plays a crucial role in the evolution of a galaxy. Dust directly and indirectly dominates the heating and cooling of clouds and thus regulates star formation. Grain surfaces provide sites for the formation of molecular hydrogen (Hollenbach & Salpeter 1970), another key coolant. The formation of dust in the outflows from evolved stars governs the rate of enrichment of the interstellar medium (ISM) (e.g. Ferrarotti & Gail 2006). Sub-mm surveys have revealed extensive populations of dusty galaxies as far as $z = 6.4$, only 0.8 Gyr after the Big Bang (Bertoldi et al. 2003), showing that dust plays a role even in the very early Universe. The IRS on *Spitzer* has revealed fundamentally different dust chemistries in high-redshift galaxies, showing emission from polycyclic aromatic hydrocarbons (PAHs) at $z = 3.0$ (Huang et al. 2007), amorphous silicate emission at $z = 2.3$ (Teplitz et al. 2006), crystalline silicates out to $z = 0.3$ (Spoon et al. 2006), and even the possibility of amorphous alumina in a quasar wind at $z = 0.5$ (Markwick-Kemper et al. 2007).

Dust properties have evolved as the Universe has aged. A key piece of evidence is the difference in UV extinction between quasars and the Galaxy (Pitman et al. 2000). The quasars lack the 2200 Å bump attributed to carbonaceous dust. Dust evolution is expected, because nearly 90% of Galactic dust forms in the winds from stars on the asymptotic giant branch (AGB) (e.g. Gehrz 1989) and this stellar population depends strongly on the age of the galaxy. The role of red supergiants (RSGs), and supernovae (SNe) is probably more important in young galaxies (e.g. Morgan & Edmunds 2003). Furthermore, metallicity influences the efficiency of dust formation (e.g. van Loon 2000).

While the dust almost certainly evolves, the specifics remain unclear. Spectra of distant galaxies are of unresolved point sources, averaging together many different dusty environments. To understand the formation efficiency and properties of the dust in harsh metal-poor environments, we must observe the individual environments which together constitute the life-cycle of dust. **The SMC is the only nearby galaxy where we can conduct such a study.**

The SMC lies at a distance of 60 kpc and has a metallicity $\sim$1/5 solar (e.g. Keller & Wood 2006). It is metal-poor and is actively forming stars. Like quasars, interstellar dust in the SMC lacks the 2200Å bump in UV extinction curves (Gordon & Clayton 1998; Pitman et al. 2000). The sensitivity of the IRS on *Spitzer* gives us the unique opportunity to analyze dust in every stage of its life cycle and understand how metallicity influences the role of dust in the evolution of a galaxy. A comprehensive spectroscopic survey of the SMC would revolutionize our understanding of dust in the early Universe. Compared to the nearby LMC, **the SMC is in danger of being neglected spectroscopically** by the *Spitzer* mission.

Existing observations highlight the importance of studying all of the dust-processing sites within a galaxy. The missing 2200Å bump in the SMC suggests an absence of C-rich dust, which contrasts with observations of evolved stars. The AGB in metal-poor environments is dominated by carbon stars (Blanco et al. 1978, 1980, Renzini & Voli 1981), and *Spitzer* spectroscopy shows

that carbon stars in the SMC are producing as much dust as their Galactic counterparts (Sloan et al. 2008). How this apparent surplus becomes a deficit in the ISM is unknown. A related problem is the role of dust in governing the mass-loss rates from evolved stars. Radiation pressure on carbon-rich dust can certainly drive the observed mass loss, but for oxygen-rich dust, the driving mechanism is uncertain (Woitke 2006). At lower metallicities, this problem becomes more acute, and this uncertainty impacts our knowledge of such parameters as enrichment and SNe rates.

We propose a comprehensive spectroscopic survey of dust in the SMC using the IRS on *Spitzer* and MIPS in SED mode. Our planned observations will fulfill three goals. First, they will provide a complete inventory of the spectral properties of dust in all of its phases, which would be a powerful tool in disentangling the integrated spectra from more distant metal-poor systems. Second, they will probe the composition, processing, and role of the dust in each stage of its life-cycle, allowing a detailed comparison to spectroscopic *Spitzer* studies of the Large Magellanic Cloud (LMC), with its slightly subsolar metallicity ($\sim$1/3 solar), and the Galaxy. Third, the proposed spectra are essential to the translation of the photometry provided by infrared surveys of the SMC into meaningful classifications of the sources. The S^{3}MC survey mapped the core of the SMC in IRAC and MIPS in Cycle 2 (Bolatto et al. 2007), and the SAGE-SMC survey (PI Gordon) is mapping a more extensive region in Cycle 4.

Spectroscopic samples in the SMC are patchy and incomplete. In all, we have 110 spectral observations of point sources, mostly of stars on the asymptotic giant branch (AGB) and supergiants (67 targets), planetary nebulae (PNe, 23), and Wolf-Rayet stars (11). In addition, several of the most extended, evolved star forming regions (SFRs) have now been mapped (the S^{4}MC program in Cycle 3, PI Bolatto). These programs are an excellent beginning to a more comprehensive understanding of the life-cycle of dust and its influence on its metal-poor host galaxy.

It is our objective to capitalize on observations already obtained and concentrate on those gaps which are essential to understanding the full evolutionary history of the dust in a metal-poor galaxy. We will focus on YSOs, compact H II regions, the diffuse ISM, post-AGB sources, and several smaller classes of important objects. Because of the importance of these data to the *Spitzer* legacy, the IRS team is allocating 62 of the 116 hours needed for this survey from its GTO time.

1.2 Young Stellar Objects

YSOs are the most underobserved population in the SMC. This omission is critical, because the physics of star formation depend on the quantity and composition of dust, which in turn depend on metallicity. To improve our understanding of how stars and disks form in metal-poor environments, we propose a comprehensive and systematic survey of 58 YSOs in the SMC. To study the impact of metallicity, we will compare our sample to the sample of $\sim$90 YSOs in the more metal-rich LMC now being observed in the Cycle-4 SAGE-SPEC IRS program and the $\sim$2000 Galactic YSOs observed by the IRS Disks Team. Our proposed sample spans the star formation process and a range in mass, from T Tauri stars to Herbig AeBe (HAeBe) stars to more massive YSOs.

The 10 and 18 μm features from amorphous silicates dominate the spectra of most YSOs. The detailed shape of these features depends on the optical depth of the circumstellar material, the temperature and size of the grains, and the relative abundances of amorphous and crystalline grains. Galactic studies show evidence that the dust grain properties evolve as the forming star evolves (e.g. Kessler-Silacci et al. 2005). Many of the spectra also show features from crystalline grains, allowing more detailed astromineralogy which probes the composition and shape distribution (e.g. Sloan et al. 2006a). Watson et al. (2008) have found that among Galactic YSOs, as dust grains grow and settle toward the disk mid-plane, the fraction of crystalline grains increases, suggesting

a time-dependent evolution of the crystalline/amorphous fraction in the dust.

In the envelopes around young embedded YSOs and in regions in the disk shadowed from direct illumination by the central star, dust grains are coated in icy mantles. The only Magellanic YSO with a published *Spitzer* spectrum is IRAS 05328−6327, a massive YSO in the LMC (van Loon et al. 2005). This spectrum shows CO_2 ice absorption at $\sim$15 μm, but no H_2O ice absorption at $\sim$6 μm. Van Loon et al. speculate that in more metal-poor environments, lower interstellar dust extinction and deeper penetration by UV radiation into the protostellar environment results in more photo-processing of the ices around YSOs. Thus, more complex ice compounds form at the expense of simple H_2O ice. Water ice is an efficient coolant, and its absence should affect the collapse of a protostellar cloud and its formation into a star. We will test how the metallicity affects the abundances of H_2O and CO_2 ices by comparing our results to the *Spitzer* samples from the LMC and the Galaxy.

In regions of the envelope and disk that are directly illuminated by the central star, dust grains are heated and icy mantles evaporated. In the Galaxy, about 8% of T Tauri stars and more than 50% of HAeBe stars show PAH emission features (Geers et al. 2006, Acke & van den Ancker 2004). The presence or absence of PAH emission can help us infer the disk geometry (e.g. inner walls or holes and the degree of flaring; Keller et al. 2008). Some Galactic HAeBe stars emit strong PAH emission and yet have little or no emission from amorphous dust, perhaps indicating that the PAHs have been released recently from the icy mantles on large dust grains (Li & Lunine 2003). In the Galaxy, PAH spectra of HAeBe stars have distinctive features different from PAHs in other environments (Sloan et al. 2005; Keller et al. 2008). We will examine the metallicity dependence of these spectral tracers of the physical properties of the disks.

1.3 Extended Regions

Dust in photodissociation regions (PDRs) around massive YSOs often dominates the emission from active star-forming galaxies. One IRS GTO program and a larger GO program in Cycle 3 (S^4MC, PI Bolatto) mapped several extended and more evolved H II regions in the SMC with the IRS. These maps allow us to track forbidden emission lines and dust properties throughout these regions, so that we can study the impact of massive stars on the dust in the ISM. In particular, we can study PAH destruction in these regions. The deficiency of PAHs below metallicities $\sim$1/5 solar is well documented (e.g. Engelbracht et al. 2005; Wu et al. 2006). PAHs play a critical role in the physics of the ISM, making it important to understand the mechanism behind their destruction in metal-poor environments. The most likely suspect is the hardness and intensity of the radiation field, but that point remains unclear.

Our proposed observations concentrate on three classes of extended regions underrepresented in the current database: compact H II regions, quiescent molecular clouds, and supernova remnants (SNRs). Studying these environments will complete our database of the building blocks of galaxies and illustrate the interaction of dust and star formation in a range of evolutionary stages. Three of our targeted regions are to be observed in a proposed *Herschel* spectroscopic program (PI Meixner) to study the heating and cooling equilibrium in the metal-poor ISM.

Our three proposed compact H II regions include two in the Magellanic Bridge (BS 216/217 and BS 200; Bica & Schmitt 1995) and one in the main body of the SMC (N 78; Henize 1956). BS 216/217 is a compact double 24 μm source recently detected in the Cycle-4 SAGE-SMC program (PI Gordon). It is also the first molecular emission knot detected in the Bridge (Muller et al. 2003). BS 200 is also a double 24 μm source, recently detected in CO (Mizuno et al. 2006). The Bridge is even more metal-poor than the SMC ($\sim$ 1/20 vs. 1/5 $Z_\odot$; Rolleston et al. 1999), making

it an extreme environment for star formation. In addition to these targets, we can map two nearby ultracompact sources (Bridge A and F) in under an hour. Our third compact H II region is N 78 in the northern Bar. It contains a handful of late O and early B stars and several bright 8 μm filaments. It is small, isolated, and easily separated from its surroundings, giving it a well-defined radiation field and simple geometry which are straightforward to model (compared to the S^{4}MC sources).

We also propose to observe a quiescent CO cloud identified in the NANTEN survey (Mizuno et al. 2001) and the isolated SNR 0104−72.3 (Mathewson et al. 1984). Leroy et al. (2007) found that the CO cloud has an unusually low far-IR/CO ratio, making it a good candidate for the study of very cold dust (e.g. Galliano et al. 2005). SNR 0104−72.3 is a compact, ring-shaped remnant in the S^{3}MC IRAC and 24 μm images and was recently detected by the Akari mission (Koo et al. 2007). It is probably a 10,000-year-old Type Ia SNR. Its warm continuum distinguishes it from the first SNR detected by *Spitzer* in the SMC (Stanimirović et al. 2005). Studying SNRs will help resolve the question of how much dust SNe produce in the early Universe (e.g. Dwek et al. 2007).

1.4 Smaller Samples

Evolved Stars — Previous samples in the SMC have concentrated on evolved stars, are dominated by carbon stars, and have left some critical holes. Stars in clusters are particularly important, because they have known metallicities and ages (and therefore masses on the AGB). Supergiants contribute ∼10% of the dust ejected into the ISM, but only four have been observed in the SMC. We will expand this sample in order to search for dependencies of dust properties with metallicity. We are also observing two luminous blue variables to compare to similar objects in the LMC which show strong crystalline silicate features in their spectra (Kastner et al. 2006). Finally, we will examine a sample of AGB stars with optically thin dust shells. Similar Galactic sources often show alumina-rich dust, instead of silicates, but in the SMC, aluminum abundance is reduced, which we anticipate will lead to the production of different pre-silicate grains. These observations will help constrain the dust condensation sequence in the outflows from evolved stars.

Post-AGB Sources — The existing samples of SMC spectra from *Spitzer* include only one post-AGB object. This badly undersampled evolutionary stage gives us the opportunity to study circumstellar dust after the conclusion of the superwind phase and before the ionized region and surrounding PDR dominate the IR spectrum. The dust in C-rich objects is in transition from amorphous carbon to PAHs, resulting in spectra with molecular absorption from acetylene and more complex hydrocarbons (e.g. Cernicharo et al. 1999; Bernard-Salas et al. 2006). MSX SMC 029, the only post-AGB object in the SMC with a *Spitzer* spectrum, also shows an unusual PAH spectrum which might indicate that the PAHs are still embedded in an aliphatic matrix (Sloan et al. 2007). Silicate-dominated post-AGB objects can be equally fascinating because the dust is often trapped in a disk, where it is annealed until it shows crystalline emission features, allowing a detailed study of the dust composition. This dust can even survive while the central star evolves into a C-rich object (e.g. HD 44179 and IRAS 09425−6040; Waters et al. 1996; Molster et al. 2001).

Planetary Nebulae — Only two of the 23 PNe observed in the SMC are O-rich. We will observe three PNe. Two are O-rich, and the third has well-constrained stellar parameters (but an unknown C/O ratio). Our O-rich targets will help fill a gap in the current sample.

The Diffuse ISM — Our sample includes three lines of sight in the diffuse ISM, one of which shows the 2200Å bump in its UV extinction curve, which is rare in the SMC. The two comparison sightlines will allow an examination of how the PAH emission spectrum in these regions varies depending on the UV extinction curve, in order to constrain the carrier of the 2200Å bump.

2 Technical Plan

2.1 The IRS Sample

We have chosen targets from the available literature and by using the S^{3}MC catalog to identify some sources based on their positions in color-color and color-magnitude space. Figure 1 illustrates how the colors and magnitudes of our sample compare to previous SMC samples. As shown, we are probing a mostly unobserved population of dusty sources.

YSOs — 58 targets (30.1 hrs). Our sample is from the S^{3}MC catalog and includes embedded YSOs ($\sim$50%) and objects with near- and mid-IR colors resembling Galactic HAeBe stars ($\sim$40%) and T Tauri stars ($\sim$10%). The sample divides roughly evenly between sources with and without strong Hα emission, an indicator of active disk accretion and/or winds. We have enough sources in each YSO category to draw statistically significant conclusions about spectral trends as functions of mass and evolutionary state and to compare them to their LMC and Galactic counterparts. We have obtained near- and mid-IR spectra and photometry for 31 YSOs, confirming their status as embedded YSOs. We are currently planning follow-up observations for more of the YSOs in our sample.

Extended regions — 7 regions (35.8 hrs). Sec. 1.3 describes how we selected our sample of extended regions in the SMC and the Bridge. The two ultracompact sources take only 0.9 hrs combined.

Evolved Stars — 30 targets (25.0 hrs). Our proposed sample includes 11 optically thin candidates, chosen on the basis of their 8 μm magnitudes and J$-$K and [8]$-$[24] colors (11.9 hrs). We will also observe three carbon stars in the cluster Kron 3, which has an age of 5 Gyr and a metallicity $\sim 0.1 Z_{\odot}$ (Girardi & Marigo 2007) (3.4 hrs), seven bright oxygen-rich stars in the young cluster NGC 330 (5.1 hrs), seven supergiants (2.1 hrs), and two luminous blue variables (2.5 hrs).

Post-AGB — 15 targets (4.6 hrs). We selected these targets based on identifications in the literature and by searching the S^{3}MC catalog for double-peaked infrared SEDs.

PNe — 3 targets (4.4 hrs).

Diffuse ISM — 3 lines of sight in the diffuse ISM, plus one offset position (7.0 hrs).

2.2 IRS Observing Strategy

We will observe all point sources using the Short-Low (SL) and Long-Low (LL) modules of the IRS, which provides sufficient wavelength coverage and resolution for the expected solid state features and molecular bands. All point sources will be observed with the standard staring mode, with the source observed in two nod positions in each aperture. We will match integration times in the two apertures of each module so that each spectral image will have three available background images, giving needed flexibility in the crowded regions of the SMC.

We have carefully designed the peak-up strategy to deal with the complexity of SMC. We have vetted all self-PU and offset PU targets for bright neighbors to avoid false peak-ups. We have chosen to use high-accuracy peak-up to ensure that the sources are well-centered in the SL slits.

Integration times will produce a S/N ratio of 100 in SL at 8 μm and a S/N of 60 in LL at 24 μm. We will need to study spectral features of $\sim$10% contrast, and in those cases, the resulting S/N will be 10 per pixel in SL and 6 in LL. We have relaxed the S/N requirements for the faintest targets in our sample to keep our total time request reasonable. To save further observing time, most sources with flux densities less than $\sim$1 mJy at 24 μm will be observed in SL only, or in a few cases, with SL and LL2.

The mapping observations of six extended sources will use slit steps of 1.85" in SL and 5.08" in LL. The redundancy will ensure that we can construct sufficiently sampled data cubes. The integration times in each position in the maps produce sensitivities $\sim 0.1-0.4$ mJy ($0.3-1$ MJy sr^{-1}) for the SL array, and $\sim 0.3-0.7$ mJy ($0.1-0.3$ MJy sr^{-1}) for the LL array. For faint extended emission our sensitivity will be considerably better, as we can average over several spatial resolution elements. In the brighter peaks in the SFRs, the S/N ratio will reach $\sim$100, even though the flux will remain considerably below the saturation limit. Thus, these large-scale maps will reveal the structure of both the bright sources and the extended emission surrounding them. We have verified this strategy with the Cycle-3 mapping program of extended H II regions in the SMC (the S^{4}MC program).

2.3 MIPS-SED Mode

We have selected a sample of 15 targets, including 11 YSOs, 2 red supergiants, 1 AGB object, and 1 PN, to observe in the MIPS-SED mode to obtain spectra from 55 to 96 μm and sample the cold dust. For the YSOs, this mode provides important constraints on the geometry of the circumstellar dust distribution. In post-AGB objects and PNe it probes the mass lost in the superwind phase on the AGB. In massive evolved stars it allows assessment of the time variation in dust production over the past 10^{3-4} years. The water ice band at 60 μm in YSOs will help to further constrain the temperature structure of the dust cloud and reveal differences in chemistry (Hoogzaad et al. 2002). In addition, the [0 I] 63 μm and [O III] 88 μm lines are important coolants in PDRs.

We chose targets for MIPS-SED from sources detected in the S^{3}MC survey in all IRAC bands and MIPS bands 1 and 2. Thus we know their 70-μm flux densities and have sufficient information at shorter wavelengths to analyze their properties. YSOs are selected predominantly from the proposed IRS sample, while evolved objects and additional objects are also selected from identifications in the literature and archived IRS spectroscopy.

The integrations will produce a S/N ratio of 30 per pixel, except for the PN and AGB source, which are somewhat fainter. In those cases, we have lowered the S/N goal to 5 per pixel to keep the integration times reasonable. Most sources will be observed in 10-s integrations, except for the brightest, which use 3-s integrations to avoid saturation. Chop throws are based on the 70 μm maps. Total integration time for 15 targets is 7.8 hours.

2.4 Data Reduction and Analysis

We have assembled a large team to process and analyze the proposed spectral database. The PI, G. Sloan, will supervise the extraction and calibration of point-source IRS spectra, with assistance from K. Kraemer and J. Bernard-Salas. R. Indebetouw and V. Lebouteiller will concentrate on the mapping data of extended regions, and J. van Loon will focus on the MIPS-SED data. For the analysis of the resulting products, we have divided our team into several smaller teams: *YSOs* — J. van Loon, J. Oliveira, L. Keller, J. Simon, M. Sewilo; *Evolved stars* — P. Wood, K. Kraemer, R. Blum, E. Lagadec, M. Marengo, K. Volk, S. van Dyk; *Post-AGB objects and PNe* — J. Bernard-Salas, M. Matsuura, J. Hora, M. Cohen; *The ISM and SFRs* — A. Bolatto, R. Indebetouw, V. Lebouteiller, K. Sandstrom, C. Bot, A. Li, S. Madden; *Overview* — G. Sloan, A. Zijlstra, A. Tielens, M. Meixner, F. Markwick-Kemper, K. Gordon.

The reduction of point-source IRS spectra will follow the standard Cornell algorithm (e.g. Sloan et al. 2006b). We use a combination of software from the SPICE package provided by the SSC, the SMART package written at Cornell, and custom software developed by team members.

We are experimenting with optimal extraction algorithms, as provided in SPICE and under development at Cornell. We are hopeful that these will improve the S/N for the faintest sources by $\sim$30% (a factor *not* included in our estimates).

We will use multiple methods to analyze the dust features in the spectra, depending on the chemistry. Amorphous silicates and related grains will dominate the observed spectral features. For emission spectra from evolved stars, we will apply the classification method introduced by Sloan & Price (1995, 1998), which quickly determine the relative contributions from amorphous silicate and amorphous alumina grains. Many of the sources we have selected will show crystalline emission features, which allow us to perform more detailed astromineralogy to study the relative contributions from silica (SiO_2), pyroxenes ([Mg,Fe]SiO_3), and olivines ([Mg,Fe]$_2SiO_4$), and within these species, the Mg/Fe ratio. To perform this analysis, we will use the dust samples studied by the Jena group (e.g. Jäger et al. 1998, 2003; Begemann et al. 1997; Fabian et al. 2001), and the Koike et al. group in Japan (e.g. Koike et al. 1995, 2003; Chihara et al. 2002). We will also explore the effects of grain shape and size, using techniques applied by Sloan et al. (2006a) and Kessler-Silacci et al. (2005). We will compare these data to spectra of similar Galactic sources, using the SWS Atlas (Sloan et al. 2003).

For any carbon-rich sources in our sample, we will apply the Manchester Method (described by Sloan et al. 2006b and Zijlstra et al. 2006), which efficiently measures the amount of amorphous carbon, the dust mass-loss rate, and the relative contributions of SiC and MgS dust and molecular species like C_2H_2. For those carbon-rich sources exposed to hotter radiation fields and showing PAH emission features, we will apply the classification method of Peeters et al. (2002), which is based on the relative positions of the various C–C modes between 6.2 and 8.2 μm. Recent work by Sloan et al. (2007) has revealed that the positions of all of the PAH emission features shift to longer wavelengths as the radiation field grows cooler, probably because the PAHs are mixed with increasing amounts of aliphatic sidegroups and chains.

To study the YSOs, we will use ground-based observations to extend the spectral information into the near-IR and model the spectral energy distributions (SEDs). To estimate the disk properties, we will compare our SEDs to a grid of models from multiple teams (Robitaille et al. 2006, 2007; D'Alessio et al. 2006; Calvet et al. 2008). Furlan et al. (2006) recently introduced a spectral indexing method using the continuum at 6, 13, and 30 μm to gauge the relative contributions of the warm and cool dust continua of T Tauri stars and compare to the models. The HAeBe stars will likely show PAHs, which we will analyze as described above. Watson et al. (2008) have added a series of crystalline dust measurements, providing a simple means of examining the degree of processing and dust geometry for a large sample.

For the evolved stars with their simpler geometries, we will apply radiative transfer models to the SEDs to further constrain the properties of the dust and the mass-loss process. P. Wood will obtain near-infrared photometry (JHKL) and optical spectroscopy from Siding Spring Observatory of many of our sources, as close to simultaneously with the *Spitzer* observations as possible.

We will use the CUBISM and PAHFIT software packages to reduce and interpret the IRS maps, along with additional software developed by the S^{4}MC Team for spectral extraction and cross-calibration with IRAC and MIPS.

We can apply all of the above methods not just to the SMC, but also to comparison data of similar targets in the Galaxy and the LMC, as observed by the *Infrared Space Observatory* and *Spitzer*. This combination of data with three distinct metallicities will allow for powerful studies of how dust properties depend on metallicity.

3 Legacy Data Products Plan

This is not a Legacy proposal.

4 Figures and Tables

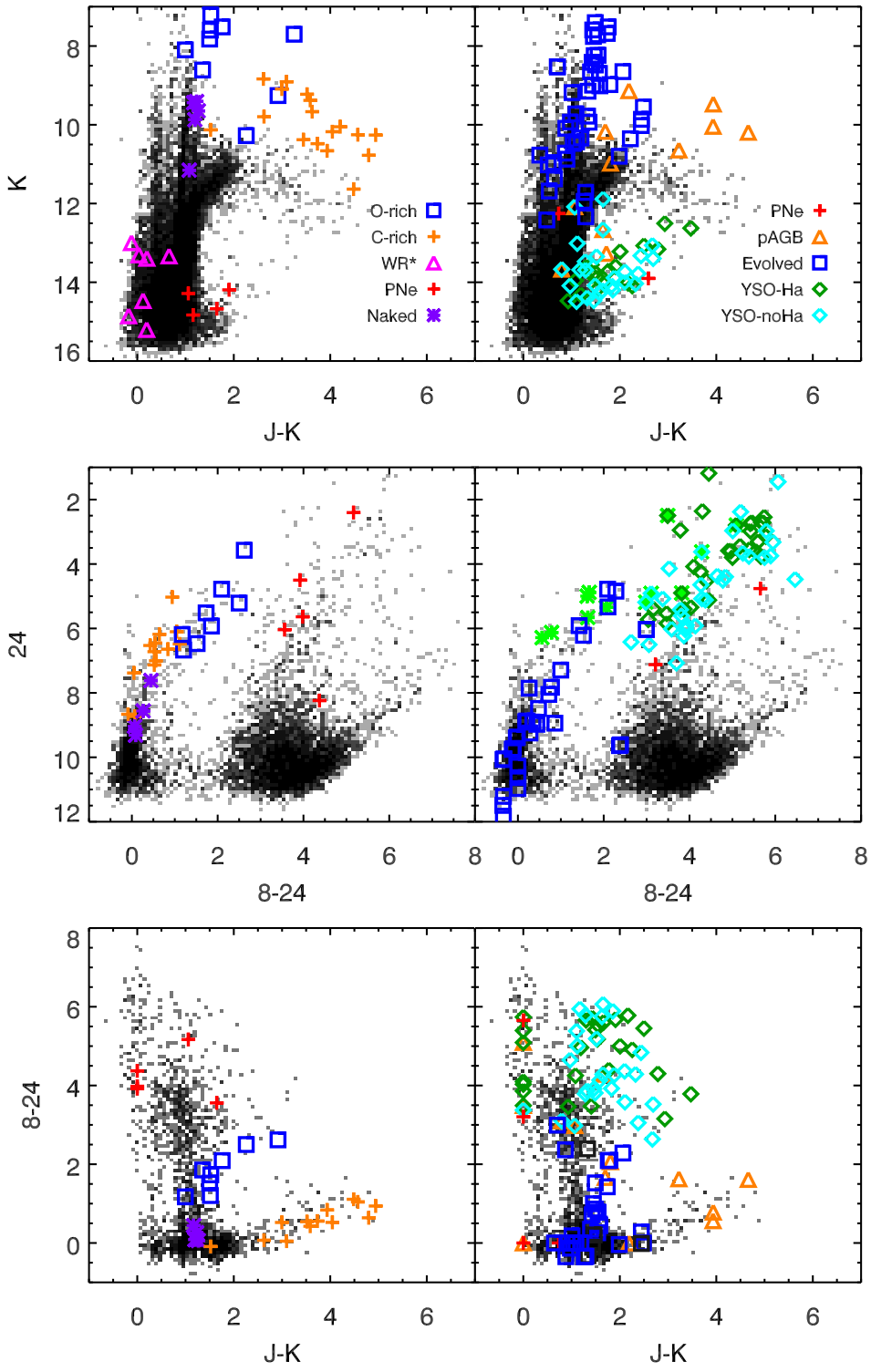

Figure 1: Color-magnitude and color-color diagrams illustrating the spectroscopic samples in the SMC (colored symbols) and the S^{3}MC sample (in black and gray; Bolatto et al. 2007). **Previous samples are to the left; the proposed sample is to the right.**

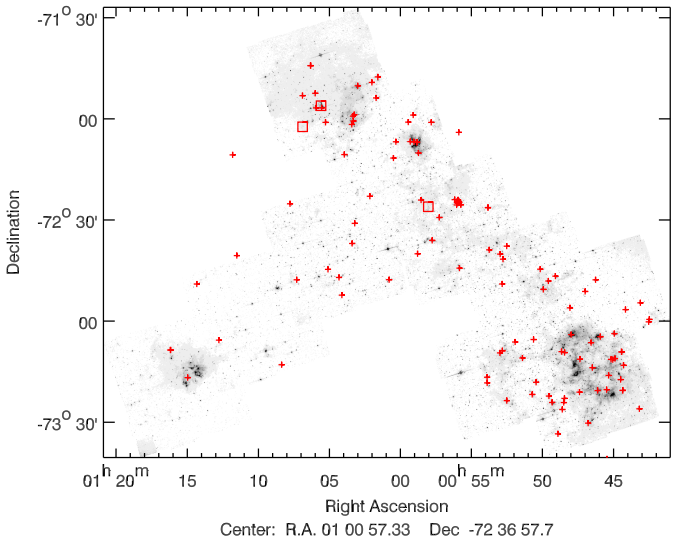

Figure 2: The 8 μm map of the SMC from the S^{3}MC survey, with our proposed targets superimposed. Squares mark mapping regions. Some sources are outside this map.

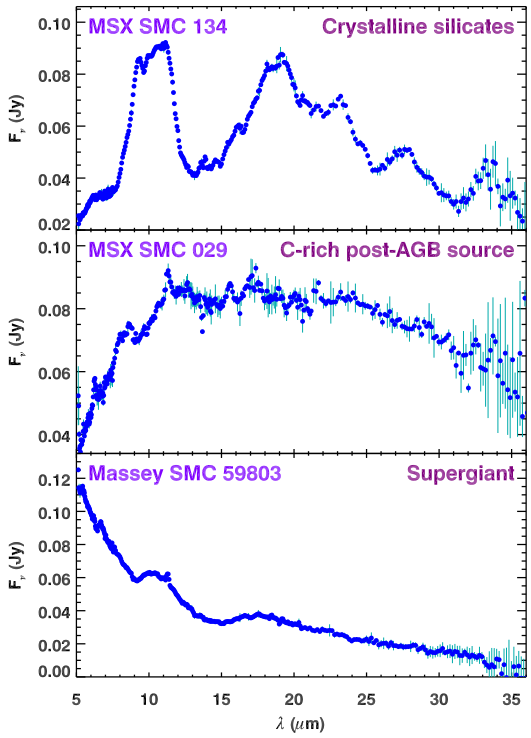

Figure 3: Three spectra from other SMC programs. The top spectrum shows strong emission features form crystalline silicates at 19.5, 23, 28, and 33 μm. The middle spectrum shows PAH emission at 6.2, 8, 8.5, 11.3, and 17 μm, in addition to acetylene absorption at 13.7 μm (Kraemer et al. 2006). The bottom spectrum, from an O-rich supergiant, also shows PAH emission at 11.3 μm.

5 Observation Summary Table

Table 1: IRS Staring observations

Target S3MC #	Other Name	Position (J2000)	$F_{8\ \mu m}$ (mJy)	$F_{24\ \mu m}$ (mJy)	SL ($N_{ramps} \times t_{int}$)	LL
11567	JO 01	00h43m12.86s -72d59m58.3s	22.8	298.9	2x60	3x6
30293	JO 02	00h44m51.87s -72d57m34.2s	34.8	588.0	3x14	3x6
36505	JO 04	00h45m21.26s -73d12m18.7s	12.0	32.7	3x60	4x30
42456	JO 05	00h45m47.51s -73d21m42.4s	12.5	49.4	3x60	2x30
50607	JO 06	00h46m24.45s -73d22m07.1s	34.3	166.6	3x14	3x6
56896	JO 07	00h46m51.72s -73d15m25.3s	20.1	36.7	2x60	3x30
80699	JO 08	00h48m25.83s -73d05m57.3s	28.3	589.0	4x14	3x6
85001	JO 09	00h48m41.78s -73d26m15.3s	10.9	222.5	4x60	3x6
90241	JO 10	00h49m01.64s -73d11m09.6s	31.2	685.0	4x14	3x6
101156	JO 11	00h49m44.57s -73d24m32.8s	16.1	43.6	2x60	3x30
114474	JO 12	00h50m40.25s -73d20m37.0s	9.6	63.9	4x60	3x14
115171	JO 13	00h50m43.24s -72d46m56.2s	27.3	587.0	4x14	3x6
118610	JO 14	00h50m58.09s -73d07m56.8s	17.4	110.7	2x60	3x6
144830	JO 15	00h52m38.84s -73d26m23.9s	35.1	571.3	3x14	3x6
158896	JO 16	00h53m25.36s -72d42m53.2s	24.2	260.7	2x60	3x6
170098	JO 17	00h54m02.31s -73d21m18.6s	129.7	472.4	3x6	3x6
170445	JO 18	00h54m03.36s -73d19m38.4s	138.9	812.4	3x6	3x6
202375	JO 21	00h56m06.50s -72d47m22.7s	14.0	256.8	3x60	3x6
226455	JO 22	00h57m57.11s -72d39m15.4s	19.4	216.6	2x60	3x6
228420	JO 23	00h58m06.41s -72d04m07.3s	17.6	341.0	2x60	3x6
256836	JO 24	01h00m22.32s -72d09m58.1s	11.4	51.9	3x60	2x30
272662	JO 25	01h01m31.70s -71d50m40.3s	28.0	459.6	4x14	3x6
291584	JO 26	01h02m48.54s -71d53m18.0s	16.9	271.5	2x60	3x6
295993	JO 27	01h03m06.14s -72d03m44.0s	12.8	49.7	3x60	2x30
324738	JO 28	01h05m07.26s -71d59m42.7s	357.9	2401.0	3x6	3x6
329936	JO 29	01h05m30.71s -71d55m21.3s	25.6	262.6	2x60	3x6
347808	JO 30	01h06m59.67s -72d50m43.1s	24.4	49.7	2x60	2x30
394191	JO 31	01h14m39.38s -73d18m29.3s	25.8	144.1	2x60	3x6
11878	LK 225	00h43m14.78s -73d00m42.7s	17.3	394.9	2x60	3x6
18912	LK 229	00h43m53.83s -72d55m14.9s	9.7	17.9	4x60	3x120
38574	LK 213	00h45m30.15s -73d12m41.1s	15.8	127.4	2x60	3x6
38732	LK 224	00h45m30.77s -73d04m55.8s	12.4	112.7	3x60	3x6

Target S3MC #	Other Name	Position (J2000)	$F_{8\ \mu m}$ (mJy)	$F_{24\ \mu m}$ (mJy)	SL ($N_{ramps} \times t_{int}$)	LL ($N_{ramps} \times t_{int}$)
41455	LK 210	00h45m42.95s -73d17m26.4s	6.7	27.3	8x60	6x30
51112	LK 222	00h46m26.82s -73d06m05.0s	9.8	216.6	4x60	3x6
57798	LK 200	00h46m55.68s -73d31m58.4s	11.5	66.4	3x60	3x14
59484	LK 220	00h47m02.85s -73d08m00.3s	6.1	30.7	8x60	4x30
83562	LK 227	00h48m36.44s -72d58m00.9s	60.0	795.8	2x14	3x6
84425	LK 204	00h48m39.64s -73d25m01.0s	55.1	157.8	2x14	3x6
86931	LK 217	00h48m49.04s -73d11m23.6s	5.9	23.1	10x60	2x120
97470	LK 202	00h49m30.12s -73d26m23.4s	14.1	223.4	3x60	3x6
100259	LK 231	00h49m41.27s -72d48m48.6s	20.1	463.5	2x60	3x6
111393	LK 230	00h50m27.21s -72d52m55.1s	15.3	19.3	2x60	3x120
117712	LK 206	00h50m54.19s -73d24m16.9s	17.5	99.0	2x60	2x14
129029	LK 212	00h51m40.58s -73d13m34.0s	2.7	115.6	12x60	3x6
152305	LK 216	00h53m03.83s -73d11m37.5s	7.2	29.5	6x60	6x30
155257	LK 215	00h53m13.38s -73d12m17.6s	9.0	226.4	6x60	3x6
155323	LK 234	00h53m13.56s -72d44m22.2s	12.6	335.2	3x60	3x6
220777	LK 237	00h57m30.07s -72d32m24.5s	41.4	464.5	3x14	3x6
236080	LK 240	00h58m42.82s -72d27m16.8s	63.4	1881.6	2x14	3x6
239883	LK 242	00h59m00.33s -72d10m05.2s	13.3	48.6	3x60	2x30
240361	LK 241	00h59m02.52s -72d10m07.4s	13.0	124.5	3x60	3x6
242496	LK 243	00h59m12.20s -72d09m58.6s	26.7	66.5	2x60	3x14
243308	LK 247	00h59m16.08s -72d02m00.2s	9.3	28.0	6x60	6x30
274262	LK 249	01h01m38.44s -71d56m55.7s	10.9	40.8	4x60	3x30
296319	LK 246	01h03m07.53s -72d02m18.1s	17.6	245.0	2x60	3x6
308876	LK 228	01h03m58.79s -72d55m32.5s	3.2	10.6	12x60	8x120
329440	LK 248	01h05m28.62s -71d59m42.8s	7.6	31.5	6x60	4x30
340160	LK 250	01h06m19.57s -71d55m59.2s	10.3	64.1	4x60	3x14
28079	2M J004441-7321	00h44m41.05s -73d21m36.4s	34.6	60.0	3x14	3x14
31234	LIN 60	00h44m56.30s -73d10m11.8s	258.5	717.4	3x6	3x6
69602	MSX SMC 069	00h47m44.55s -73d13m07.6s	110.4	25.3	3x6	6x30
89695	IRAS F00471-7352	00h48m59.46s -73d35m38.3s	145.4	71.5	3x6	3x14
172299	LIN 250	00h54m09.49s -72d41m43.4s	154.6	79.6	3x6	2x14
175179	LIN 254	00h54m19.16s -72d29m09.6s	45.0	544.9	2x14	3x6
258866	MSX SMC 212	01h00m31.70s -72d14m49.1s	116.8	21.9	3x6	2x120
304821	MSX SMC 234	01h03m42.35s -72d13m42.8s	69.6	51.8	2x14	2x30
321441	2M J010453-7204	01h04m53.21s -72d04m03.9s	77.7	38.8	3x6	3x30
333357	2M J010546-7147	01h05m46.43s -71d47m05.4s	39.7	77.3	3x14	2x14
390385	IRAS F01122-7306	01h13m41.16s -72d50m50.0s	56.2	167.6	2x14	3x6
397643	LIN 517	01h15m42.82s -73d09m59.4s	44.1	253.8	2x14	3x6
202333	[KVS00] MIR1	00h56m06.38s -72d28m28.1s	20.9	78.3	2x60	2x14
...	IRAS 00350-7436	00h36m59.71s -74d19m50.3s	150.0	300.0	3x6	3x6
...	MSX SMC 192	01h33m33.94s -72d44m05.4s	63.0	39.0	2x14	3x30
13882	2M J004326-7326	00h43m26.44s -73d26m43.6s	9.9	1.4	4x60	8x120
28791	2M J004444-7314	00h44m44.58s -73d14m08.1s	16.7	2.9	2x60	8x120
86193	PMMR 23	00h48m46.44s -73d28m20.6s	34.3	7.3	3x14	8x120
107009	RAW 594	00h50m08.46s -72d50m20.4s	8.5	1.8	6x60	8x120
155318	2M J005314-7251	00h53m13.56s -72d51m45.1s	10.9	1.8	4x60	8x120

Target S3MC #	Other Name	Position (J2000)	$F_{8\ \mu m}$ (mJy)	$F_{24\ \mu m}$ (mJy)	SL ($N_{ramps} \times t_{int}$)	LL
280458	PMMR 132	01h02m04.05s -72d26m11.0s	7.7	1.9	6x60	8x120
295538	PMMR 141	01h03m04.28s -72d34m13.1s	36.3	5.1	3x14	8x120
298358	PMMR 145	01h03m15.38s -72d40m12.4s	12.7	2.0	3x60	8x120
311530	HV 11464	01h04m09.41s -72d50m15.9s	20.0	4.3	2x60	8x120
321424	Massey SMC 60447	01h04m53.11s -72d47m49.2s	23.1	5.3	2x60	8x120
384393	RAW 1640	01h12m23.30s -73d07m50.3s	7.4	1.7	6x60	8x120
...	Kron 3 W24	00h24m50.27s -72d47m47.0s	3.0	0.3	12x60	8x120
...	Kron 3 W54	00h24m46.93s -72d47m54.3s	2.4	0.2	12x60	8x120
...	Kron 3 MA1	00h25m00.26s -72d46m25.3s	1.7	0.1	12x60	8x120
203760	S3MC 203760	00h56m12.85s -72d27m46.7s	3.8	0.4	12x60	...
203963	S3MC 203963	00h56m13.88s -72d27m32.5s	8.6	0.7	6x60	...
204111	S3MC 204111	00h56m14.55s -72d27m42.5s	15.6	2.1	2x60	...
204676	S3MC 204676	00h56m17.07s -72d27m35.1s	5.2	0.6	12x60	...
204803	S3MC 204803	00h56m17.53s -72d27m04.3s	12.1	1.3	3x60	...
205083	S3MC 205083	00h56m18.80s -72d27m47.6s	1.1	1.1	12x60	...
205104	S3MC 205104	00h56m19.02s -72d28m08.3s	9.5	1.0	4x60	...
351225	HD 6884	01h07m18.18s -72d28m03.5s	15.7	27.6	2x60	6x30
245457	HD 5980	00h59m26.57s -72d09m54.1s	8.6	1.0	6x60	8x120
...	HV 12956	01h09m02.25s -71d24m10.2s	277.0	421.0	3x6	3x6
...	RMC 50	01h44m03.86s -74d40m49.8s	357.0	590.0	3x6	3x6
30415	S3MC 30415	00h44m52.52s -73d18m26.3s	69.7	61.9	2x14	3x14
262457	S3MC 262457	01h00m48.09s -72d51m02.1s	114.1	87.2	3x6	2x14
359870	S3MC 359870	01h08m10.37s -73d15m52.9s	90.3	82.4	3x6	2x14
247216	Massey SMC 46662	00h59m34.95s -72d04m06.8s	51.3	23.3	2x14	2x120
278036	Massey SMC 52334	01h01m54.15s -71d52m19.0s	30.9	8.6	4x14	8x120
295070	Massey SMC 55188	01h03m02.43s -72d01m53.0s	74.2	30.8	3x6	4x30
207709	SMP SMC 21	00h56m30.89s -72d27m01.6s	4.4	88.9	10x60	8x30
205199	MGPN SMC 8	00h56m19.59s -72d06m58.5s	...	187.2	12x60	12x30
...	SMP SMC 4	00h40m46.21s -75d16m20.8s	3.0	25.0	10x60	10x30
68163	AzV 23	00h47m38.86s -73d22m54.1s	1.8	...	8x60	...
238721	AzV 214	00h58m54.74s -72d13m17.4s	0.5	...	24x60	...
...	AzV 456	01h10m55.74s -72d42m56.2s	3.0	...	24x60	...
...	AzV sky	01h38m03.00s -78d58m00.0s	...	...	24x60	...

There are 108.4 hrs total in IRS AORs and 7.8 hrs total in MIPS AORs.

Table 2: IRS Mapping Observations

Target	Position (J2000)	SL ramps ($N \times t$)	LL ramps ($N \times t$)	SL map width (")	LL map width (")	Total time (h)
NANTEN cloud	00h58m14.00s −72d29m15.0s	1×60	1×30	80	60	6.9
SNR 0104-72.3	01h06m21.85s −72d05m14.5s	1×60	1×30	80	60	6.9
N78	01h05m09.31s −71d59m05.0s	1×14	1×14	150	200	4.9
off positions	01h38m03.00s −78d58m00.0s	various	various	...	...	0.5
Bridge A	01h43m54.22s −74d32m24.9s	1×60	1×14	13	15	0.5
BS 200/Bridge B1	01h49m41.90s −74d36m54.3s	2×60	1×14	70	70	4.1
BS 200/Bridge B2	01h49m26.12s −74d39m09.5s	2×60	1×14	70	70	4.1
BS 216/217 (C1)	01h56m54.70s −74d15m42.0s	2×60	1×14	70	70	4.1
BS 216/217 (C2)	01h56m37.00s −74d15m55.0s	2×60	1×14	70	70	4.1
Bridge F	02h14m40.75s −74d21m27.0s	1×60	1×14	13	15	0.5

Table 3: MIPS-SED Observations

S3MC	Other name	Position (J2000)	$F_{70\ \mu m}$ (mJy)	Total time (s)
30293	IRAS 00429−7313	00h44m51.86s −72d57m34.2s	1250	1251
31234	IRAS 00430−7326	00h44m56.30s −73d10m11.6s	6910	774
50607	jo06	00h46m24.46s −73d22m07.3s	1150	1405
84425	lk204	00h48m39.62s −73d25m00.8s	481	3704
112218	IRAS 00486−7308	00h50m30.62s −72d51m29.9s	117	3704
127934	Jacoby SMC 17	00h51m36.55s −73d20m17.2s	103	3704
137535	BMB-B 75	00h52m12.82s −73d08m52.8s	463	3704
170098	jo17	00h54m02.30s −73d21m18.7s	1450	1097
170445	jo18	00h54m03.36s −73d19m38.3s	2340	789
324738	jo28	01h05m07.25s −71d59m42.7s	6880	774
329821	IRAS 01039−7305	01h05m30.22s −72d49m53.8s	2270	789
333967	IRAS 01042−7215	01h05m49.30s −71d59m48.8s	1300	1251
347808	jo30	01h06m59.66s −72d50m43.1s	425	3704
366860	N81	01h09m12.67s −73d11m38.4s	8870	774
394191	jo31	01h14m39.38s −73d18m29.2s	4190	789

6 References

Acke, B. & van den Ancker, M. E. 2004, A&A, 426, 151
Begemann, B., et al. 1997, ApJ, 476, 199
Bertoldi, F., et al. 2003, A&A, 406, L55
Bernard-Salas, J., et al. 2006, ApJ, 652, L29
Bica, E. L. D. & Schmitt, H. R. 1995, ApJS, 101, 41
Blanco, B. M., et al. 1978, Nature, 271, 638
Blanco, B. M., et al. 1980, ApJ, 242, 938
Bolatto, A. D., et al. 2007, ApJ, 644, 212
Calvet, N., et al. 2008, in preparation
Cernicharo, J., et al. 2001, ApJ, 546, L123
Chihara, H., et al. 2002, A&A, 391, 267
D'Alessio, P., et al. 2006, ApJ, 638, 314
Dwek, E., et al. 2007, arXiv 0711.1170
Engelbracht, C. W., et al. 2005, ApJ, 628, L29
Fabian, D., et al. 2001, A&A, 378, 228
Ferrarotti, A. S. & Gail, H.-P. 2006, A&A, 447, 553
Furlan, E., et al. 2006, ApJS, 165, 568
Galliano, F., et al. 2005, A&A, 434, 867
Geers, V. C., et al. 2006, A&A, 459, 545
Gehrz, R. D., 1989, in IAU Symp. 135, 445
Girardi, L. & Marigo, P. 2007, A&A, 462, 237
Gordon, K. & Clayton, G. C. 1998, ApJ, 500, 816
Henize, K. 1956, ApJS, 2, 31
Hollenbach, D. J. & Salpeter, E. E. 1970, J. Chem. Phys. 53, 79
Hoogzaad, S. N., et al. 2002, A&A, 389, 547
Huang, J.-S., et al. 2007, ApJ, L69
Jäger, C., et al. 1998, A&A, 339, 904
Jäger, C., et al. 2003, A&A, 408, 193
Kastner, J. H., et al. 2006, ApJ, 638, L29
Keller, L. D., et al. 2008, ApJ, submitted
Keller, S. C. & Wood, P. R. 2006, ApJ, 642, 834
Kessler-Silacci, J. E., et al. 2005, 622, 404
Koike, C., et al. 1995, Icarus, 114, 203
Koike, C., et al. 2003, A&A, 399, 1101
Koo, B.-C., et al. 2007, PASJ, in press (arXiv 0704.0706)
Kraemer, K. E., et al. 2006, ApJ, 652, L25
Leroy, A., et al. 2007, ApJ, 658, 1027
Li, A. & Lunine, J. I. 2003, ApJ, 594, 987
Markwick-Kemper, F., et al. 2007 ApJ, 668, L107
Mathewson, D. S., et al. 1984, ApJS, 55, 189
Mizuno, N., et al. 2001, PASJ, 53, L45
Mizuno, N., et al. 2006, ApJ, 643, L107
Molster, F. J., et al. 2001, A&A, 366, 923
Morgan, H. L. & Edmunds, M. G. 2003, MNRAS, 343, 427
Muller, E., et al. 2003 MNRAS, 338, 609
Peeters, E., et al. 2002, A&A, 390, 1089
Pitman, K. M., et al. 2000, PASP, 112, 537
Renzini, A. & Voli, M. 1981, A&A, 94, 175
Robitaille, T. P., et al. 2006, ApJS, 167, 256
Robitaille, T. P., et al. 2007, ApJS, 169, 328
Rolleston, W. R. J., et al. 1999, A&A, 348, 728
Sloan, G. C., et al. 2003, ApJS, 147, 379
Sloan, G. C., et al. 2005, ApJ., 632, 956
Sloan, G. C., et al. 2006a, ApJ, 632, 956
Sloan, G. C., et al. 2006b, ApJ, 645, 1118
Sloan, G. C., et al. 2007, ApJ, 664, 1144
Sloan, G. C., et al. 2008, in preparation
Sloan, G. C. & Price, S. D., 1995, ApJ, 451, 758
Sloan, G. C. & Price, S. D., 1998, ApJS, 119, 141
Spoon, H. W. W., et al. 2006, ApJ, 638, 759
Stanimirović, S., et al. 2005, ApJ, 632, L103
Teplitz, H. I., et al. 2006, ApJ, 638, L1
van Loon, J. Th. 2000, A&A, 354, 125
van Loon, J. Th. 2005, MNRAS, 364, 71
Waters, L. B. F. M., et al. 1996, A&A, 315, 361
Watson, D. M., et al. 2008, ApJS, submitted (arXiv 0704.1518)
Woitke, P. 2006, A&A, 452, 537
Wu, Y., et al. 2006, ApJ, 639, 157
Zijlstra, et al. 2006, MNRAS, 370, 1961

7 Brief Resume/Bibliography

G. Sloan (PhD Wyoming 1992) specializes in infrared spectroscopy of molecules, dust and complex hydrocarbons in stellar photospheres, circumstellar shells and the ISM. Since 2001, he has been a member of the IRS Team at Cornell, where he helped develop the calibration plan and data processing and analysis tools for the IRS. He has been a lead author on five refereed IRS papers and an author on 30 more IRS papers (plus 3 in press or submitted).
A. Zijlstra (PhD Groningen 1989) concentrates on mass loss from evolved stars and planetary nebulae at optical, infrared, and radio wavelengths at the Univ. of Manchester.
A. Tielens (PhD Leiden 1982) is an authority on the physics and chemistry of interstellar dust and gas. He is the PI of the SAGE-SPEC Legacy program to study the LMC spectroscopically.
M. Meixner (PhD Berkeley 1993) is a full astronomer at STScI, instrument team leader on JWST, and PI of the SAGE Legacy program to study the LMC.
F. Markwick-Kemper (PhD Amsterdam 2002) is now on the faculty at the Univ. of Manchester, where she studies the formation and evolution of dust within and beyond the Galaxy.
K. Gordon (PhD Toledo 1997) specializes in interstellar dust in Galactic and extragalactic environments, is PI of the SAGE-SMC mapping program, and is now at STScI.
J. van Loon (PhD Amsterdam 1999) is on the faculty at the Univ. of Keele and studies infrared stellar populations and the interaction of dust and stellar evolution.
P. Wood (PhD ANU 1974) studies pulsation and mass loss in evolved stars at Mt. Stromlo.
J. Bernard-Salas (PhD Groningen 2003) is on the IRS Team at Cornell and studies post-AGB objects, PNe, and H II regions.
A. Bolatto (PhD Boston Univ. 2001) is on the faculty of the Univ. of Maryland, PI of the S^3MC and S^4MC programs, and is studying the ISM and star formation in nearby galaxies.
R. Indebetouw (PhD Colorado 2001) studies star formation in the Galaxy and its neighborhood.
L. Keller (PhD Texas 1999) is on the faculty of Ithaca College and studies YSOs with infrared spectroscopy.
K. Kraemer (PhD Boston Univ. 1997) studies dust in many astrophysical settings at the Air Force Research Lab.
V. Lebouteiller (PhD IA Paris 2005) is on the IRS Team at Cornell and studies star formation and the chemical evolution of galaxies.
J. Oliveira (PhD Univ. Porto 2001) studies star formation and its environmental impact at Keele.

Publications (not already in Sec. 6):

Groenewegen, Wood, Sloan, et al. 2007, "Luminosities and mass-loss rates of carbon stars in the Magellanic Clouds," MNRAS, 376, 313

Kraemer, Sloan, Wood, et al. 2005, "R CrB candidates in the Small Magellanic Cloud: Observations of cold, featureless dust with the Spitzer Infrared Spectrograph," ApJ Letters, 631, L147

Lagadec, Zijlstra, Sloan, et al. 2007, "*Spitzer* mid-infrared spectra of AGB stars in the Small Magellanic Cloud," MNRAS, 376, 1270

Matsuura, Wood, Sloan, et al. 2006, "*Spitzer* observations of acetylene bands in carbon-rich AGB stars in the Large Magellanic Cloud, MNRAS, 371, 415

Meixner, Gordon, Indebetouw, et al. 2006, "*Spitzer* survey of the Large Magellanic Cloud: Surveying the Agents of a Galaxy's Evolution (SAGE). I. Overview and initial results," AJ, 132, 2268

Sloan, Charmandaris, Fajardo-Acosta, et al. 2004 "The serendipitous discovery of a debris disk around the A dwarf HD 46190," ApJ Letters, 614, L77

8 Status of Existing Spitzer Programs

PI G. Sloan is the TC for the IRS GTO MC_DUST program (PID 200, 17 hrs), which has led to one paper, with another to be submitted soon. He is a co-investigator on two Cycle 1 IRS GO programs to study the SMC (PID 3277; 17 hrs) and both the SMC and LMC (PID 3505; 31 hrs), which have led to eight papers, with more in preparation. He is also leading three small IRS GTO programs in Cycle 3 (total 9 hrs) and is an investigator on two Cycle 3 IRS GO programs, one to study S stars in the Galaxy (PID 30737, 20 hrs), and the other to study evolved stars in nearby Local Group galaxies (PID 30333, 33 hrs). We have 4 papers in preparation and 3 more planned. He is PI of 2 ongoing Cycle 4 programs, to study circumstellar shells in globular clusters (PID 40111, 19 hrs) and to obtain a sample of M giant spectra (PID 40112, 5 hrs). Observations are underway.

The large ensemble of co-investigators on this project is involved in quite a few *Spitzer* programs. The table below lists only those which are relevant to this proposal; it is still a *long* list. In the "Papers" column, "out" refers to papers published or in press in refereed journals. Many of those described as "in prep" should be submitted by the time you are reading these very words!

Table 4: Relevant Spitzer Programs

Investigator	PID	Type	T (h)	Subject	Status	Papers
Sloan (TC)	200	GTO-0	17	MC_DUST spectra	complete	1 out, 1 in prep
Bernard-Salas (TC)	103	GTO-0	11	Mag. Cloud PNe	complete	3 out, 1 in prep
Markwick-Kemper	1094	DDT-1	16	LMC spectra	complete	1 out, 1 planned
Wood	3505	GO-1	31	Mag. Cloud spectra	complete	5 out, 1 planned
Kraemer (TC)	3277	GO-1	17	SMC spectra	complete	3 out, 1 in prep
Markwick-Kemper	3591	GO-1	6	LMC spectra	complete	1 in prep
Bolatto	3316	GO-1	46	S^3MC - SMC maps	complete	4 out, 1 in prep
Zijlstra	20357	GO-2	22	Local Group spectra	complete	1 out
Meixner	20203	GO-2	511	SAGE - LMC maps	complete	2 out, 4 submitted
van Loon	20648	GO-2	18	ω Cen maps	complete	1 out, 1 in prep
Sloan (TC)	30332	GTO-3	6	Mag. Cloud spectra	complete	see PID 200
Sloan (TC)	30345	GTO-3	1	14 μm features	complete	see PID 200, 3277
Sloan (TC)	30355	GTO-3	1	SMC spectra	complete	1 planned
Sloan (TC)	30737	GO-3	20	S star spectra	complete	2 in prep, 1 planned
Zijlstra	30333	GO-3	33	Local Group spectra	complete	2 in prep, 2 planned
Bernard-Salas	30652	GO-3	5	Halo PNe	complete	1 in prep, 1 planned
Bolatto	30491	GO-3	106	S^4MC spec. maps	complete	2 in prep
Sloan	40111	GTO-4	19	Glob. cluster dust	ongoing	planning
Sloan	40112	GTO-4	5	M giant spectra	ongoing	1 planned
Bernard-Salas	40035	GTO-4	18	Outer disk PNe	not started	planning
Bolatto	40132	GO-4	8	I Zw 18	ongoing	planning
Meixner	40010	GO-4	16	SN dust	not started	planning
Tielens	40159	GO-4	224	LMC spectra	not started	planning
Gordon	40245	GO-4	285	SAGE-SMC maps	ongoing	1 in prep, planning
IRS programs		0–3	292		complete	14 out, 18 more
non-IRS programs		0–3	575		complete	7 out, 6 more

9 Proprietary Period Modification

There are no modifications to the proprietary period.

10 Justification of Duplicate Observations

There are no duplicate observations.

11 Justification of Targets of Opportunity

There are no ToO observations.

12 Justification of Scheduling Constraints

While we have no official scheduling constraints, the panel should be aware that the SMC is not observable from *Spitzer* from late December, 2008 to late May, 2009. Given the current best estimate for the exhaustion of cryogens on 16 April, 2009 and a back-log of Cycle 4 observations to complete when Cycle 5 begins in July, 2008, scheduling of this program is tightly constrained already. Not only must this proposal be successful, but it must receive a high priority to be executed!